

Low Temperature Densification and Electrochemical Properties of $\text{Sm}_{0.16}\text{Ce}_{0.84}\text{O}_{1.92}$ electrolyte by Zn Doping

Tao Yang¹, Qian Hu¹, Fang Yang¹, Fang Yang¹, Hao Fang¹, Chunhua Zhao^{1,2,*}

¹ Key Laboratory for Ultrafine Materials of Ministry of Education, School of Materials Science and Engineering, East China University of Science and Technology, Shanghai 200237, China

² CAS Key Laboratory of Materials for Energy Conversion, Shanghai 200050, PR China

*E-mail: zhaochh@ecust.edu.cn

Received: 14 April 2016 / Accepted: 22 May 2016 / Published: 4 June 2016

$\text{Zn}_x\text{Sm}_{0.16}\text{Ce}_{0.84-x}\text{O}_{1.92-x}$ ($0 \leq x \leq 0.1$) oxides were prepared by solid state reaction. Zn as sintering additive and dopant was investigated. Zn can be doped into the fluorite structure at $x \leq 0.04$, and at $x = 0.1$ the secondary phase ZnO can be identified. The sintering activity increased with increasing of x . At 1200 °C, the relative density runned up to 95% at $x \geq 0.02$, while the relative density of Zn-free composition reached only 75%. In order to get the relative density above 95%, the Zn-free sample need to be sintered at 1400 °C. The conductivity can also be improved by appropriate Zn doping.

Keywords: $\text{Zn}_x\text{Sm}_{0.16}\text{Ce}_{0.84-x}\text{O}_{1.92-x}$; densification; sintering; electrical properties

1. INTRODUCTION

In the past decades, solid oxide fuel cells (SOFC) have been of great interest for the next generation energy conversion system due to their high energy efficiency and environmental friendship. Zirconia and ceria based electrolytes are the two most conventional electrolyte materials. Compared with zirconia based electrolytes, ceria based electrolytes have higher ionic conductivity, which can lower SOFC's operation temperature to 600 °C [1, 2]. It is hard to fabricate highly dense ceria based electrolytes below 1400 °C. A higher temperature of 1400-1600 °C is usually required which will lead to several disadvantages such as the partial reduction of Ce^{4+} to Ce^{3+} above 1200 °C and undesirable reactions between the cell components [3].

The sintering behavior can be improved by two ways: using nano-scaled powders and adding sintering additives. Hydrothermally prepared $\text{Ce}_{1-x}\text{Sm}_x\text{O}_{2-x/2}$ (SDC) powders with the small particle size of 40-68 nm can be sintered into highly dense ceramics at 1400 °C [4]. The SDC powders prepared by a modified sol-gel method have been sintered to a higher relative density at relatively lower

sintering temperature of 1300 °C [5]. The small particle size of the starting powders requires a flexible process, which increases the cost and limits their commercial application. The doping of appropriate sintering aids can also decrease the sintering temperature of ceramics effectively. Some transition metal oxides, such as CuO, CoO_x, and Fe₂O₃ are very effective sintering aids for the reduction of the sintering temperature of ceria based electrolytes. A reduction of 200 to 300 °C in densification sintering temperature was observed [6,7]. Negatively, additions of these variable-valence cations might increase the electronic conductivities.

In this paper, Zn was chosen as the sintering additive of Sm_{0.16}Ce_{0.84}O_{1.92}. Firstly, Zn was proven to be an ideal sintering aid for some ceramics. By adding 4 mol% ZnO additive, the densification temperature of BaSn_{0.75}Y_{0.25}O_{3-δ} compounds can be successfully reduced from 1600 to 1300 °C [8]. Huang et al. investigated the sintering temperature of (1-x)Li₂TiO_{3-x}ZnO (x = 0.0–0.5). They showed that ZnO can lower the sintering temperature from 1300 to 1150 °C with x increasing to 0.5 [9]. Secondly, Zn has only one valance, Zn²⁺, the doping of Zn into the fluorite structure can't produce the electronic conductivity.

2. EXPERIMENTAL

2.1 Fabrication of Zn_xSm_{0.16}Ce_{0.84-x}O_{1.92-x}

Powders of Zn_xSm_{0.16}Ce_{0.84-x}O_{1.92-x} (0 ≤ x ≤ 0.1) were prepared by solid state reaction [10]. Analytical-grade cerium acetate hydrate Ce(CH₃COO)₃·1.5H₂O, samarium acetate hydrate Sm(CH₃COO)₃·H₂O, zinc acetate Zn(CH₃COO)₂, and oxalic acid H₂C₂O₄·2H₂O were used as starting materials. A mixture of these acetates and oxalic acid with a molar ratio of total metal ions: oxalic acid of 1:1.5 was milled at room temperature for 5 h in a polyethylene container using zirconia balls as the milling medium and ethanol as the dispersion agent until a uniform paste was gained, which indicated the starting materials have thoroughly reacted. Then the precursor mixture was dried, pulverized, sieved, and then calcined in furnace at 800 °C for 5 h.

The as-obtained powders were blended with an organic binder (PVA, n=1750, Shanghai Chemical Reagent Co. Ltd., China) and sieved. Disk-shaped powder compacts of diameter 5 mm and thickness 3 mm were formed by uniaxial pressing at 200 MPa. The powder compacts were heated in air to 400 °C at a rate of 100 °C/h and kept at that temperature for 2 h to remove the organic binder, and sintered at different temperatures and kept at that temperature for 5 h for sintering, and then furnace-cooled to room temperature.

2.2 Measurements

The sintered ceramics were analyzed using XRD with a Philips X-Pert diffractometer using Cu Kα radiation (λ = 0.15418 nm). The lattice parameters were fitted by the Powdercell software using the least squares method. The density ρ was measured using Archimedes method. The relative density ρ_{rel} was determined according to the formula ρ_{rel}=ρ/ρ_{th}, where ρ_{th} is the theoretical density calculated

from the lattice parameter as obtained from the XRD result and ρ is the real density. The microstructures of the sintered ceramics were observed with a Hitachi X-600 scanning electron microscope (SEM).

For measuring the electrical conductivity, the two opposite sides of the sintered disks were polished and coated with silver paste, heated at 850 °C for metallization and quenched to room temperature. Gold wires were attached as electrode leads. The electrical conductivities were measured from 400 to 800 °C by a two-probe technique with an Agilent34401A digital multimeter.

3. RESULTS AND DISCUSSION

The X-ray patterns of $\text{Zn}_x\text{Sm}_{0.16}\text{Ce}_{0.84-x}\text{O}_{1.92-x}$ ($0 \leq x \leq 0.1$) sintered at 1200 °C are presented in Fig.1. A tetragonal fluorite structure (JCPDS: 82-1243) is formed at a low Zn content ($x \leq 0.04$) [11]. At $x = 0.1$ the secondary phase of ZnO can be identified between 30°-40° in the pattern. From the XRD results, we can see that a certain amount of Zn can be doped into the fluorite lattice.

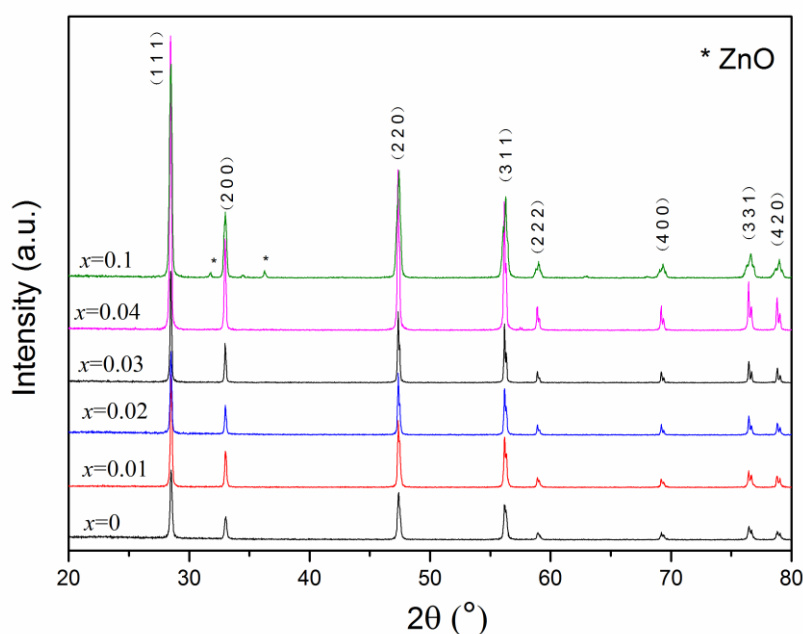


Figure 1. The X-ray patterns of $\text{Zn}_x\text{Sm}_{0.16}\text{Ce}_{0.84-x}\text{O}_{1.92-x}$ ($0 \leq x \leq 0.1$) sintered at 1200 °C.

The values of lattice parameter a , theoretical density, and real density of $\text{Zn}_x\text{Sm}_{0.16}\text{Ce}_{0.84-x}\text{O}_{1.92-x}$ ($0 \leq x \leq 0.04$) calculated from the X-ray data analysis as a function of x are shown in Table.1. The lattice constant a is almost constant with the increase of the Zn doping. The lattice parameter a is determined by the ionic radii and the oxygen vacancy concentration. The effective ionic coordination number (8) radius for Zn^{2+} , Sm^{3+} , and Ce^{4+} are 90, 107.9, and 114.3 pm, respectively [12]. When ZnO

is dissolved in the lattice, the reaction (using Kroeger-Vink notation) can be expressed as: $ZnO \xrightarrow{CeO_2} Zn_{Ce}^{\bullet} + O_o^{\times} + V_o^{\bullet}$. The substitute of Ce^{4+} by Zn^{2+} causes the decrease of lattice parameter a . At the same time, the production of oxygen vacancy may lead to the increase of a . The theoretical density decreases with x due to the lighter atom weight of Zn compared with Ce. The real density increases with Zn content.

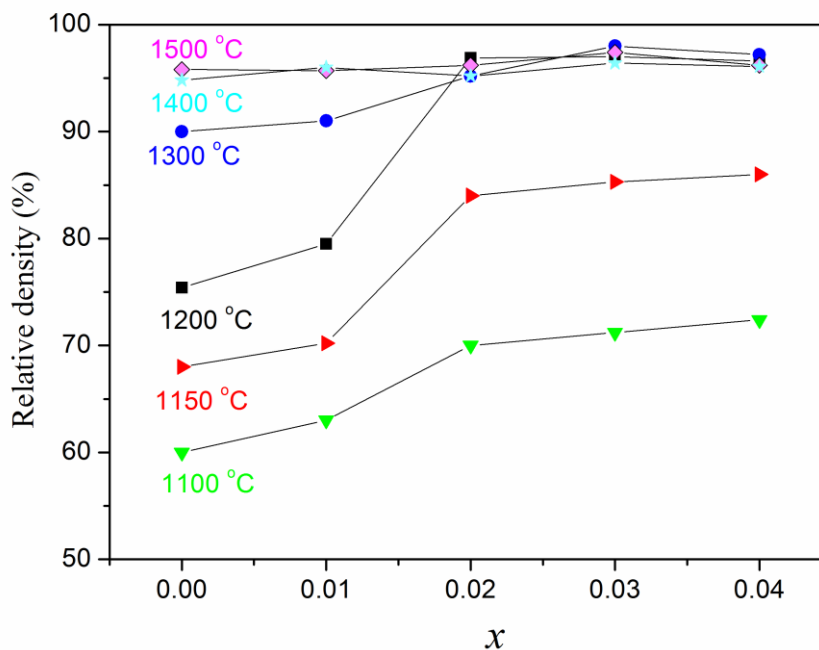
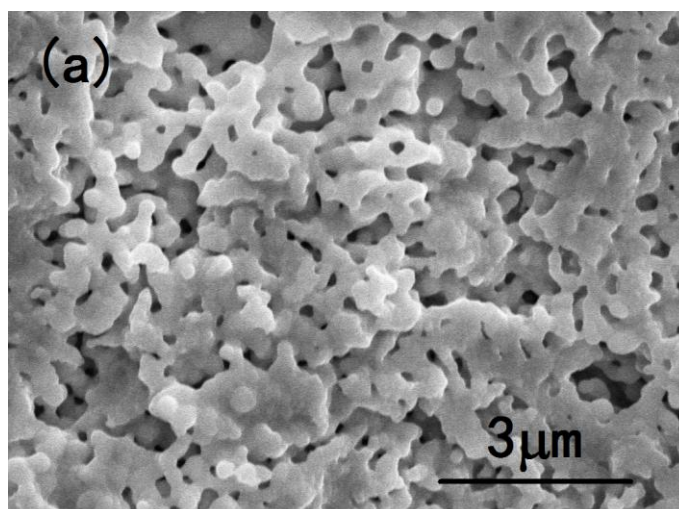


Figure 2. The relative densities of $Zn_xSm_{0.16}Ce_{0.84-x}O_{1.92-x}$ ($0 \leq x \leq 0.04$) sintered from 1100 to 1500°C.

Fig.2 shows the densification of $Zn_xSm_{0.16}Ce_{0.84-x}O_{1.92-x}$ ($0 \leq x \leq 0.04$) sintered from 1100 to 1500°C.



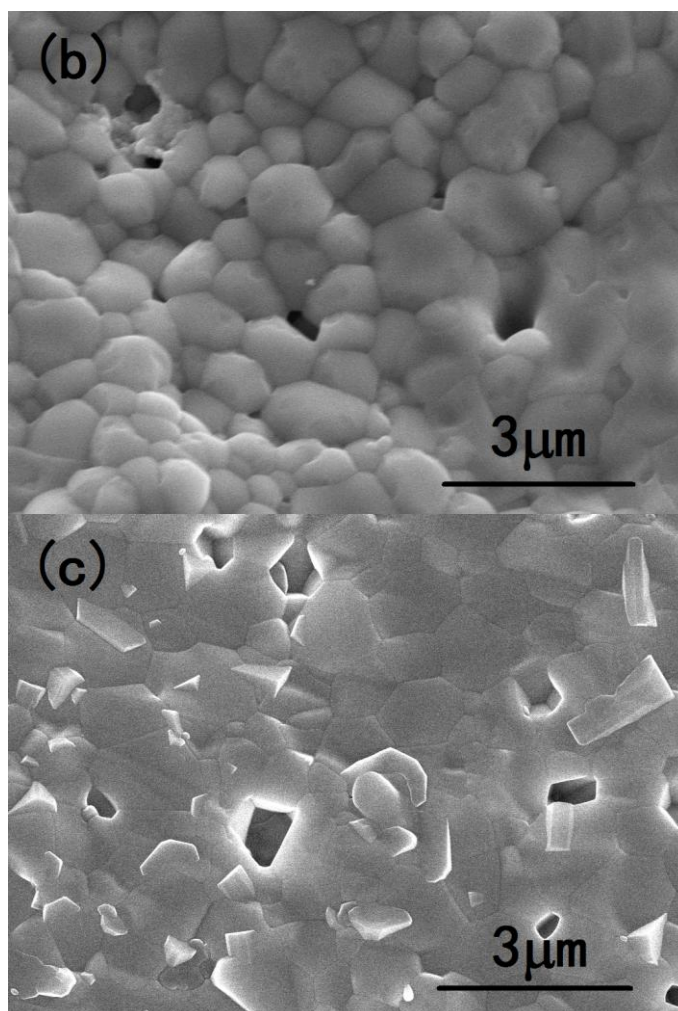


Figure 3. The cross-section SEM images of $\text{Sm}_{0.16}\text{Ce}_{0.84}\text{O}_{1.92}$ (a), $\text{Zn}_{0.02}\text{Sm}_{0.16}\text{Ce}_{0.82}\text{O}_{1.90}$ (b), and $\text{Zn}_{0.04}\text{Sm}_{0.16}\text{Ce}_{0.80}\text{O}_{1.88}$ (c) sintered at 1200 °C.

From 1100 to 1300 °C, the relative density increases with increasing of x . At 1200 °C, the relative density runs up to 95% at $x \geq 0.02$, while the relative density of Zn-free composition reaches only 75%. In order to get the relative density above 95 %, the Zn-free sample need to be sintered at 1400 °C. Above 1400 °C, all the samples have the relative densities above 95%. The microstructures of the sintered ceramics were investigated and the typical cross-section SEM images are shown in Fig. 3 and 4. At 1200 °C, Zn-free $\text{Sm}_{0.16}\text{Ce}_{0.84}\text{O}_{1.92}$ contains large number of open pores. In contrast, $\text{Zn}_{0.02}\text{Sm}_{0.16}\text{Ce}_{0.82}\text{O}_{1.90}$ and $\text{Zn}_{0.04}\text{Sm}_{0.16}\text{Ce}_{0.80}\text{O}_{1.88}$ ceramics were well sintered with few pores and grains connected to each other which were in accordance with the density measurements. The grain size increases with Zn content. The beneficial effect of Zn additive on densification of SDC is obvious. The rapid densification for the Zn-doped samples at relative lower sintering temperatures can be attributed to the formation of Zn-rich liquid phase films in the grain boundaries. The effective liquid phase diffusion under capillary action and the subsequent acceleration of mass transport via a dissolution–precipitation mechanism results in rapid densification and grain coarsening [13]. Even no Zn-rich liquid film formed, the doping of Zn can still influence the sintering process. Firstly, the melting point of $\text{Zn}_x\text{Sm}_{0.16}\text{Ce}_{0.84-x}\text{O}_{1.92-x}$ may decrease with Zn doping which will increase the sintering

activity. Secondly, the new formed vacancies and defects could accelerate the mass transport process and increase the sintering rate [14, 15]. The densification of $\text{Sm}_{0.16}\text{Ce}_{0.84}\text{O}_{1.92}$ increases a lot when it was sintered at 1300 °C, as shown in Fig. 4.

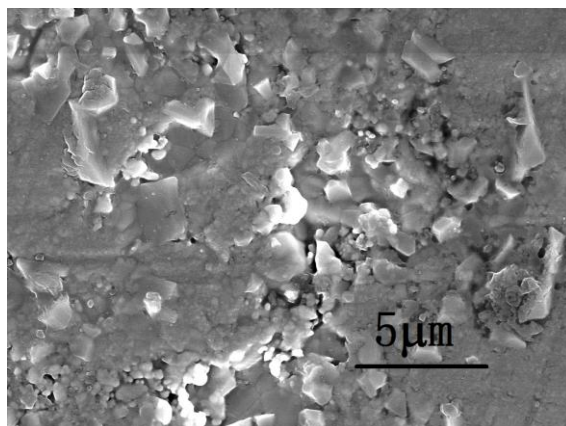


Figure 4. The cross-section SEM image of $\text{Sm}_{0.16}\text{Ce}_{0.84}\text{O}_{1.92}$ sintered at 1300 °C.

Table 1. Lattice parameter (a), theoretical density, and real density of $\text{Zn}_x\text{Sm}_{0.16}\text{Ce}_{0.84-x}\text{O}_{1.92-x}$ ($0 \leq x \leq 0.04$)

x	Lattice parameter a (Å)	Theoretical density (g/cm^3)	Real density (g/cm^3)
0	5.425	7.176	5.454
0.01	5.426	7.135	5.637
0.02	5.416	7.099	6.815
0.03	5.426	7.062	6.850
0.04	5.427	7.019	6.703

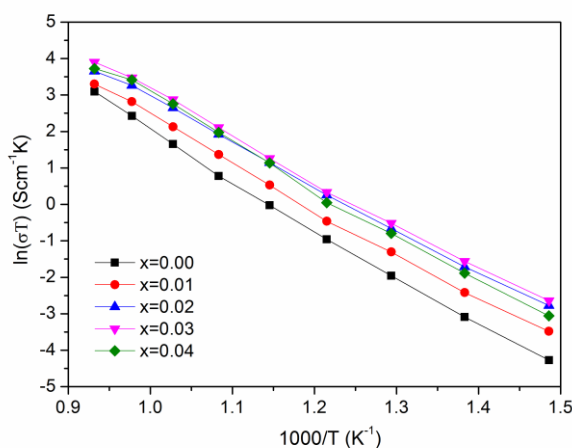


Figure 5. Arrhenius-type plots of conductivity for $\text{Zn}_x\text{Sm}_{0.16}\text{Ce}_{0.84-x}\text{O}_{1.92-x}$ ($0 \leq x \leq 0.04$) sintered at 1200 °C.

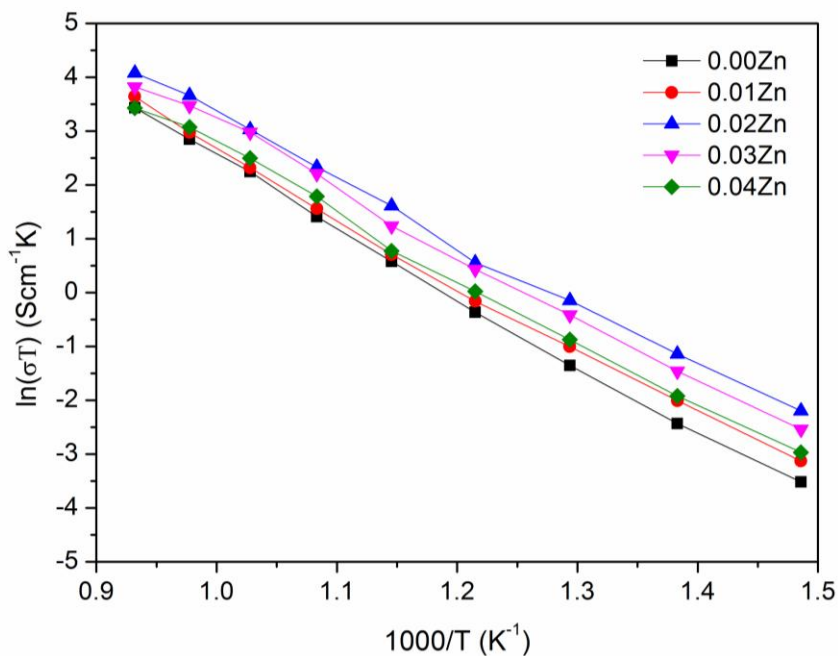


Figure 6. Arrhenius-type plots of conductivity for $Zn_xSm_{0.16}Ce_{0.84-x}O_{1.92-x}$ ($0 \leq x \leq 0.04$) sintered at 1300 °C.

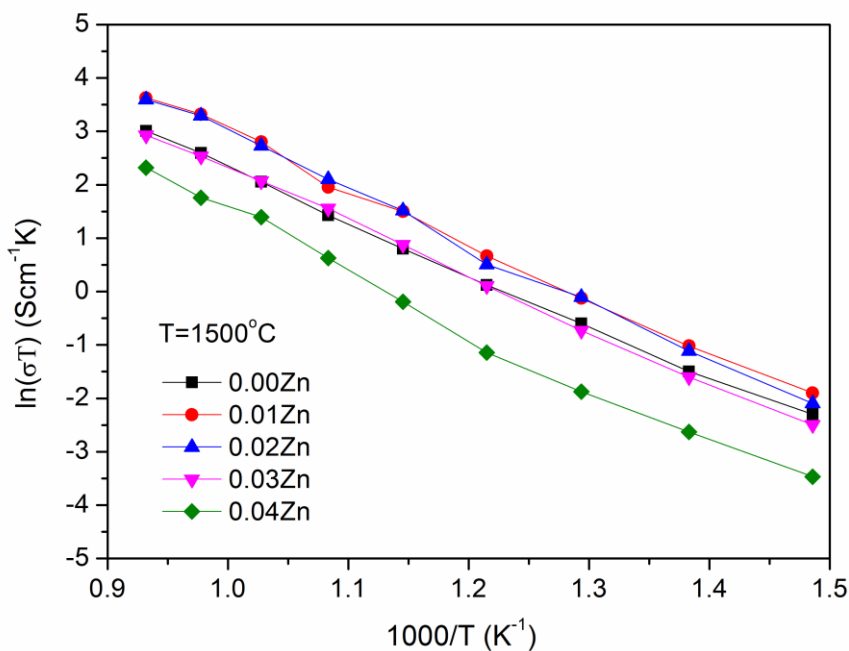
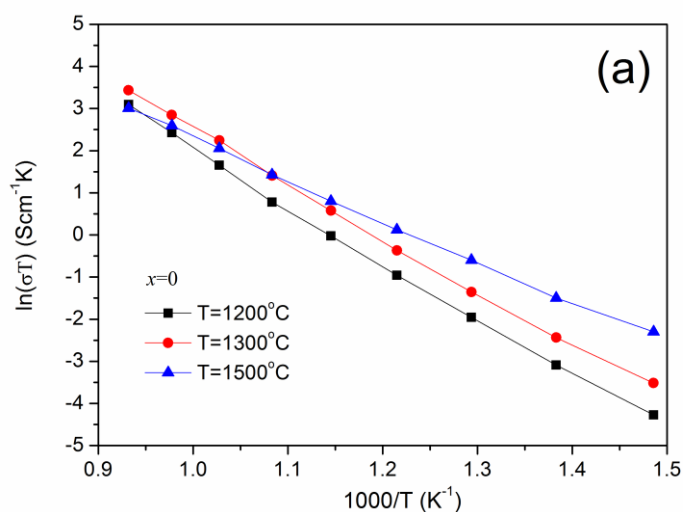


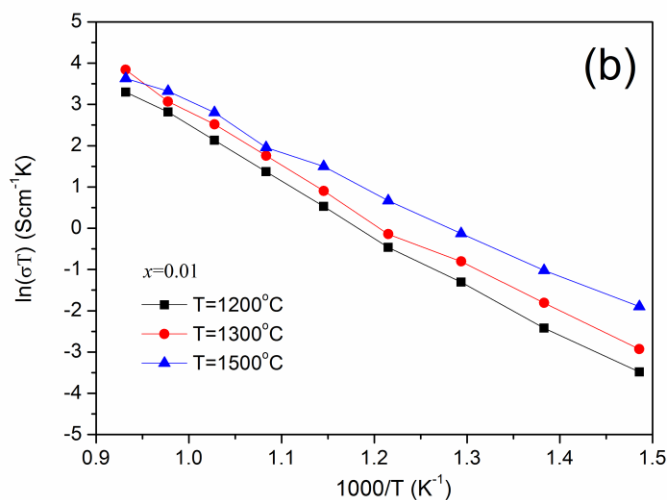
Figure 7. Arrhenius-type plots of conductivity for $Zn_xSm_{0.16}Ce_{0.84-x}O_{1.92-x}$ ($0 \leq x \leq 0.04$) sintered at 1500 °C.

Fig. 5-7 present the Arrhenius-type plots of conductivity for $Zn_xSm_{0.16}Ce_{0.84-x}O_{1.92-x}$ ($0 \leq x \leq 0.04$) sintered from 1200 to 1500 °C. The conductivity increases with Zn content from 0 to 0.03, then

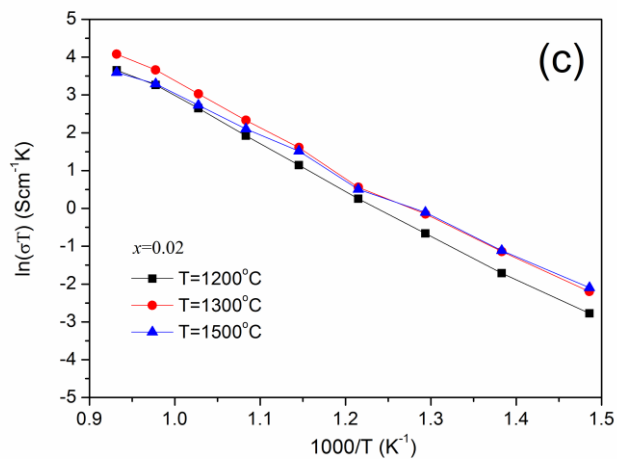
decreases a little at $x = 0.04$ when the samples are sintered at 1200 °C. The conductivity increases with Zn content from 0 to 0.02, then decreases from 0.02 to 0.04 when the samples are sintered at 1300 °C and 1500 °C. For the Ce-based electrolyte, the contribution of the electronic conductivity is negligible in air, and therefore conduction comes from the migration of oxygen ions through the oxygen vacancies that provide the migration channels [16]. Three factors can influence the conductivity: the concentration of oxygen vacancy, the density of the ceramics, and the phase structure. The oxygen vacancies increase with Zn doping which will lead to the increase in conductivity. But oxygen vacancy ordering may cause the decrease of conductivity. The increase in relative density can lead to the increase in conductivity due to the insulation of the pores [7]. The precipitation of ZnO phase can lead to the decrease in conductivity because ZnO can't transfer oxygen ions.



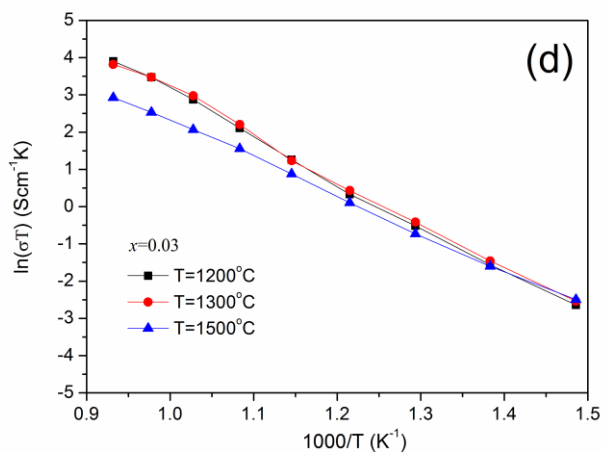
A



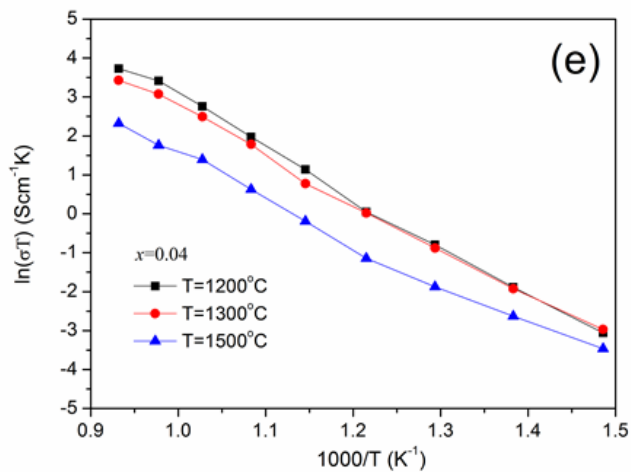
B



C



D



E

Figure 8. Arrhenius-type plots of conductivity for $\text{Zn}_x\text{Sm}_{0.16}\text{Ce}_{0.84-x}\text{O}_{1.92-x}$ ($0 \leq x \leq 0.04$) sintered at 1200°C , 1300°C and 1500°C : (a) $x = 0$, (b) $x = 0.01$, (c) $x = 0.02$, (d) $x = 0.03$, and (e) $x = 0.04$.

For all the samples, the increase in conductivity with x comes mainly from the increase in oxygen vacancy and relative density. The decrease with x comes mainly from the oxygen vacancy ordering and the precipitation of ZnO. In addition, the activation energy of $\text{Zn}_x\text{Sm}_{0.16}\text{Ce}_{0.84-x}\text{O}_{1.92-x}$ ($0 \leq x \leq 0.04$) sintered at different temperatures are shown in Table.2. In general, the activation energy decreases with Zn content from 0 to 0.03, then increases at 0.04. The activation energy decreases with increasing of sintering temperature for all the samples.

Table 2. The activation energy of $\text{Zn}_x\text{Sm}_{0.16}\text{Ce}_{0.84-x}\text{O}_{1.92-x}$ ($0 \leq x \leq 0.04$) sintered at 1200 °C, 1300 °C and 1500 °C

Sintering temperature (°C)	x				
	0	0.01	0.02	0.03	0.04
	(KJ/mol)	(KJ/mol)	(KJ/mol)	(KJ/mol)	(KJ/mol)
1200	110.8	104.1	99.1	100.7	105.5
1300	106.3	101.1	96.3	98.8	99.3
1500	81.0	85.5	87.6	83.4	89.7

The influence of sintering temperature on the electrical properties of each sample was given in Fig. 8. From 1200 to 1300 °C, we can see that the conductivity increases with increasing sintering temperature for the Zn free and $x = 0.01$ samples, as shown in Fig. 8a and b. The increase in conductivity is attributed to the increase in density. Compared with the samples sintered at 1300 °C, the sample sintered at 1500 °C have lower conductivity at high temperature and higher conductivity at low temperature due to the lower activation energy. From Fig. 8c we can see that the sintering temperature has little influence on the conductivity of $x = 0.01$ sample. From Fig. 8d and e we can see that the conductivity keeps almost the same when the $x = 0.03$ and $x = 0.04$ samples were sintered at 1200 and 1300 °C. With further increase the sintering temperature to 1500 °C, the conductivity decreases which may come from the precipitation of ZnO phase.

4. CONCLUSIONS

$\text{Zn}_x\text{Sm}_{0.16}\text{Ce}_{0.84-x}\text{O}_{1.92-x}$ ($0 \leq x \leq 1$) oxides was prepared by solid state reaction method. ZnO both as sintering aid and dopant can significantly increase the densification of ceria based electrolytes. Zn can be doped into the fluorite lattice. At 1200 °C, the relative density runed up to 95% at $x \geq 0.02$, while the relative density of Zn-free composition reached only 75%. 1400 °C was needed for the Zn-free sample to get the relative density over 95%. At the same time, Zn doping can improve the electricity of $\text{Zn}_x\text{Sm}_{0.16}\text{Ce}_{0.84-x}\text{O}_{1.92-x}$. ZnO is a good sintering additive and dopant for the Ceria based electrolytes.

ACKNOWLEDGEMENTS

This work is supported by National Natural Science Foundation of China (Grant no. 51102094), Opening Project of CAS Key Laboratory of Materials for Energy Conversion, Research Fund for the Doctoral Program of Higher Education of China (Grant no. 20110074120013), Shanghai Leading Academic Discipline Project (Grant no. B502), Shanghai Key Laboratory Project (Grant no. 08DZ2230500).

References

1. H. Sun, Y. Zhang, H. Gong, Q. Li, Y. Bu, T. Li, *Ceram. Int.* 42 (2016) 4285-4289.
2. J. Jacob, R. Bauri, *Ceram. Int.* 41 (2015) 6299-6305.
3. B. Lin, W. Sun, K. Xie, Y. Dong, D. Dong, X. Liu, J. Gao, G. Meng, *J. Alloys. Compd.* 465 (2008) 285-290.
4. W. Huang, A. P. Shuk, M. Greenblatt, *Chem. Mater.* 9 (1997) 2240-2245.
5. G. B. Jung, T. J. Huang, M. H. Huang, C. L. Chang, *J. Mater. Sci.* 36 (2001) 5839-5844.
6. Q. Lü, X. Dong, Z. Zhu, Y. Dong, *Ceram. Int.* 40 (2014) 15545-15550.
7. H. Yoshida, T. Inagaki, *J. Alloys. Compd.* 408-412 (2006) 632-636.
8. Y. Wang, A. Chesnaud, E. Bevilion, J. Yang, G. Dezanneau, *Mater. Sci. Eng. B* 176 (2011) 1178-1183.
9. C. Huang, Y. Tseng, J. Chen J, *J. Eur. Ceram. Soc.* 32 (2012) 3287-3295.
10. Y. Zhao, C. Zhao, Y. Tong, *J. Electroceram.* 31 (2013) 286-290.
11. Z. Sun, Y. Zhang, H. Gong, Q. Li, Y. Bu, T. Li, *Ceram. Int.* 42 (2016) 4285-4289.
12. Dean J A, *Lange's Handbook of Chemistry, 15th ed.*, McGraw-Hill, INC., New York, 1999.
13. C. Tseng, P. Chen, P. Lin, *J. Alloys Compd.* 632 (2015) 810-815.
14. M. Valant, D. Suvorov, R. C. Pullar, K. Sarma, N. M. Alford, *J. Eur. Ceram. Soc.* 26 (2006) 2777-2783.
15. J. Hong, S. Ida, T. Ishihara, *Solid State Ionics* 262 (2014) 374-377.
16. A. Tsoga, A. Naoumidis, D. Stöver, *Solid State Ionics* 135 (2000) 403-409.

© 2016 The Authors. Published by ESG (www.electrochemsci.org). This article is an open access article distributed under the terms and conditions of the Creative Commons Attribution license (<http://creativecommons.org/licenses/by/4.0/>).